Hindawi
Journal of Engineering
Volume 2018, Article ID 9487070, 10 pages
https://doi.org/10.1155/2018/9487070

Research Article

Effect of Flow Attack Angle for V-Wavy Plate on Flow and Heat Transfer in a Square Channel Heat Exchanger

Amnart Boonloi [1] **and Withada Jedsadaratanachai** [2]

[1] *Department of Mechanical Engineering Technology, College of Industrial Technology, King Mongkut's University of Technology North Bangkok, Bangkok 10800, Thailand*
[2] *Department of Mechanical Engineering, Faculty of Engineering, King Mongkut's Institute of Technology Ladkrabang, Bangkok 10520, Thailand*

Correspondence should be addressed to Withada Jedsadaratanachai; kjwithad@kmitl.ac.th

Received 8 May 2017; Accepted 24 October 2017; Published 30 January 2018

Academic Editor: Felix Sharipov

Effects of flow attack angles of the V-wavy plate on flow and heat transfer in a square channel heat exchanger are investigated numerically. The V-wavy plates with V-tips pointing downstream and upstream called V-Downstream and V-Upstream, respectively, are examined for the Reynolds number in the range of 3000–10,000. The finite volume method with SIMPLE algorithm is selected to solve the present problem. The numerical results are presented in terms of flow and heat transfer visualization. The thermal performance analysis is also concluded in the form of Nusselt number ratio (Nu/Nu_0), friction factor ratio (f/f_0), and thermal enhancement factor (TEF). The numerical result shows that the wavy plate can induce the swirling flow through the test section for all cases. The swirling flow disturbs the thermal boundary layer on the channel wall which is the reason for heat transfer enhancement. In range studies, the heat transfer rate increases around 3–6.5 and 2.8–6 times above the smooth channel for V-Downstream and V-Upstream, respectively. The optimum TEF is found at $\alpha = 20^\circ$ and Re = 3000 to be around 2.09 for V-Upstream case.

1. Introduction

Heat exchanger is important equipment for various industries. The thermal improvement of heat exchanger can help to save production cost and energy. The thermal improvement in the heat exchanger is separated into two methods: active and passive methods. The active method requires additional power to enhance heat transfer rate of the system. The passive method is done by installing turbulators or vortex generators in the heating/cooling system. The flow created by the vortex generators will disturb the thermal boundary layer on the heat transfer surface which is the reason for heat transfer augmentation. The passive method is worthy way to improve thermal performance in the heat exchanger when compared with active method.

The thermal performance improvement of the heat exchanger with passive method had been performed by many researchers. The V-shaped baffle/rib is a type of vortex generator which gives high effectiveness. The investigations on flow and heat transfer in heat exchanger with V-shaped baffle/rib had been presented. For examples, Kumar et al. [1] experimentally investigated heat transfer and friction loss in a solar air channel with broken V-baffle. The effects of parameters, relative baffle gap, baffle height, baffle pitch, and flow attack angle, were studied. They reported that the broken V-baffle has better performance when compared with other shapes. They also concluded that the optimums of the relative baffle gap distance, relative baffle gap width, baffle height ratio, baffle pitch ratio, and flow attack angle are around 0.67, 1, 0.5, 1.5, and 60°, respectively. Jedsadaratanachai et al. [2] numerically studied laminar flow and heat transfer in a circular tube fitted with 45° V-baffle. They indicated that the 45° V-baffle can enhance heat transfer rate higher than the smooth tube. They also summarized that the maximum thermal performance is around 3.2 at the baffle height ratio of 0.2 and 0.25 for V-Upstream and V-Downstream,

respectively. Jedsadaratanachai and Boonloi [3] presented the numerical investigation on flow and heat transfer behaviors in a square channel placed with 30° double V-baffle. The influences of baffle height and baffle pitch were investigated for Re = 100–1200. They found that the installation of the double V-baffle in the heating section performs upper heat transfer rate and thermal performance compared with the smooth square channel. Caliskan and Baskaya [4] studied the enhancement of heat transfer for the surfaces placed with V-rib. Jin et al. [5] numerically investigated flow pattern and heat transfer characteristic in a solar air heater added with staggered multiple V-shaped rib. The parameters, rib height, pitch, and attack angle, were varied. They pointed out that the maximum thermal performance is around 2.43. Deo et al. [6] reported performance analysis of a solar air heater duct roughened with multigap V-down ribs combined with staggered ribs. They showed that the maximum augmentations of the Nusselt number and thermal performance are around 3.34 and 2.45 times, respectively. Promthaisong et al. [7] selected the discrete broken V-rib to enhance heat transfer rate and thermal performance in a square channel heat exchanger. They concluded that the square channel with the discrete broken V-rib not only provides higher heat transfer rate, but also enhances pressure loss. Fang et al. [8] studied turbulent flow structure in a square channel with V-shaped rib on one wall. The flow attack angles for the V-shaped rib were compared. Maithani and Saini [9] reported the heat transfer and friction loss in a solar air heater duct with V-rib. The influences of the Reynolds number, number of gaps, relative gap width, relative roughness width, and flow attack angle were investigated experimentally. They detected that the enhancements of heat transfer rate and friction loss are around 3.6 and 3.67 times above the smooth duct. Jin et al. [10] numerically studied heat transfer and flow topology in a solar air heater duct with multi V-shaped ribs on absorber plate. They indicated that the rib in the duct provided better fluid mixing which is the cause for heat transfer enhancement.

Another interesting vortex generator is wavy surface. The wavy surface always selects improving heat transfer rate and thermal performance in fin-and-tube heat exchanger. The wavy surface can increase the strength of the flow in the heat exchanger. The combinations between wavy fin and the other types of the turbulators in the fin-and-tube heat exchanger had been reported by many researchers [11–16].

Boonloi and Jedsadaratanachai [17] numerically investigated laminar flow and heat transfer in a square channel fitted with V-wavy plate. The V-wavy plate is a combination of the vortex generators between V-shaped baffle and wavy surface. The researchers found that the V-wavy plate gives the heat transfer rate and efficiency close to the V-baffle. The production and maintenance of the V-wavy plate are more convenient than the V-shaped baffle. The optimum flow attack angle of the V-wavy plate in the heat exchanger channel for the laminar regime was concluded.

As [17], similar configuration of the heat exchanger channel inserted with V-wavy surface is tested for the turbulent regimes in the present work. The influences of the flow attack angle on heat transfer and flow structure are performed. The numerical results are reported in terms of flow and heat transfer mechanisms in the test channel. The thermal performance in the heat exchanger channel is also analyzed.

2. Physical Model and Boundary Condition

The wavy plate with square profile ($0.2H \times 0.2H$) is inserted in the middle of the square channel heat exchanger as in Figure 1. The periodic module of the numerical model is equal to the channel height (H). The flow attack angles of the wavy plate (α = 15°, 20°, 25°, 30°, 35°, 40°, 45°, 50°, 55°, and 60°) are varied for the Reynolds number in the range of 3000–10,000. The effects of arrangements for the wavy plate are studied: V-tip pointing downstream called "V-Downstream" and V-tip pointing upstream called "V-Upstream." The created domain for the square channel inserted with wavy plate is also depicted in Figure 1.

The square channel walls are set with uniform heat flux around 600 W/m^2, while the wavy plate is assumed as adiabatic wall (insulator). The inlet and outlet of the computational domain for the square channel inserted with wavy plate are set with periodic boundary. No slip wall condition is imposed for all surfaces of the numerical model.

3. Mathematical Foundation and Assumption

The tested fluid is air that keeps the thermal properties at the average bulk mean temperature. The flow and heat transfer are steady in three dimensions. The flow is turbulent and incompressible. The natural convection, radiation, viscous dissipation, and body force are not considered.

The turbulent model is realizable $k-\varepsilon$ with enhanced wall treatment as follows:

$$\begin{aligned}
&\frac{\partial}{\partial t}(\rho k) + \frac{\partial}{\partial x_j}\left(\rho k u_j\right) \\
&\quad = \frac{\partial}{\partial x_j}\left[\left(\mu + \frac{\mu_t}{\sigma_k}\right)\frac{\partial k}{\partial x_j}\right] + G_k + G_b - \rho\varepsilon - Y_M + S_k, \\
&\frac{\partial}{\partial t}(\rho \varepsilon) + \frac{\partial}{\partial x_j}\left(\rho \varepsilon u_j\right) \\
&\quad = \frac{\partial}{\partial x_j}\left[\left(\mu + \frac{\mu_t}{\sigma_\varepsilon}\right)\frac{\partial \varepsilon}{\partial x_j}\right] + \rho C_1 S\varepsilon - \rho C_2 \frac{\varepsilon^2}{k + \sqrt{\upsilon\varepsilon}} \\
&\qquad + C_{1\varepsilon}\frac{\varepsilon}{k} C_{3\varepsilon} G_b + S_\varepsilon.
\end{aligned} \tag{1}$$

where

$$\begin{aligned}
C_1 &= \max\left[0.43, \frac{\eta}{\eta + 5}\right], \\
\eta &= S\frac{k}{\varepsilon}, \\
S &= \sqrt{2S_{ij}S_{ij}};
\end{aligned} \tag{2}$$

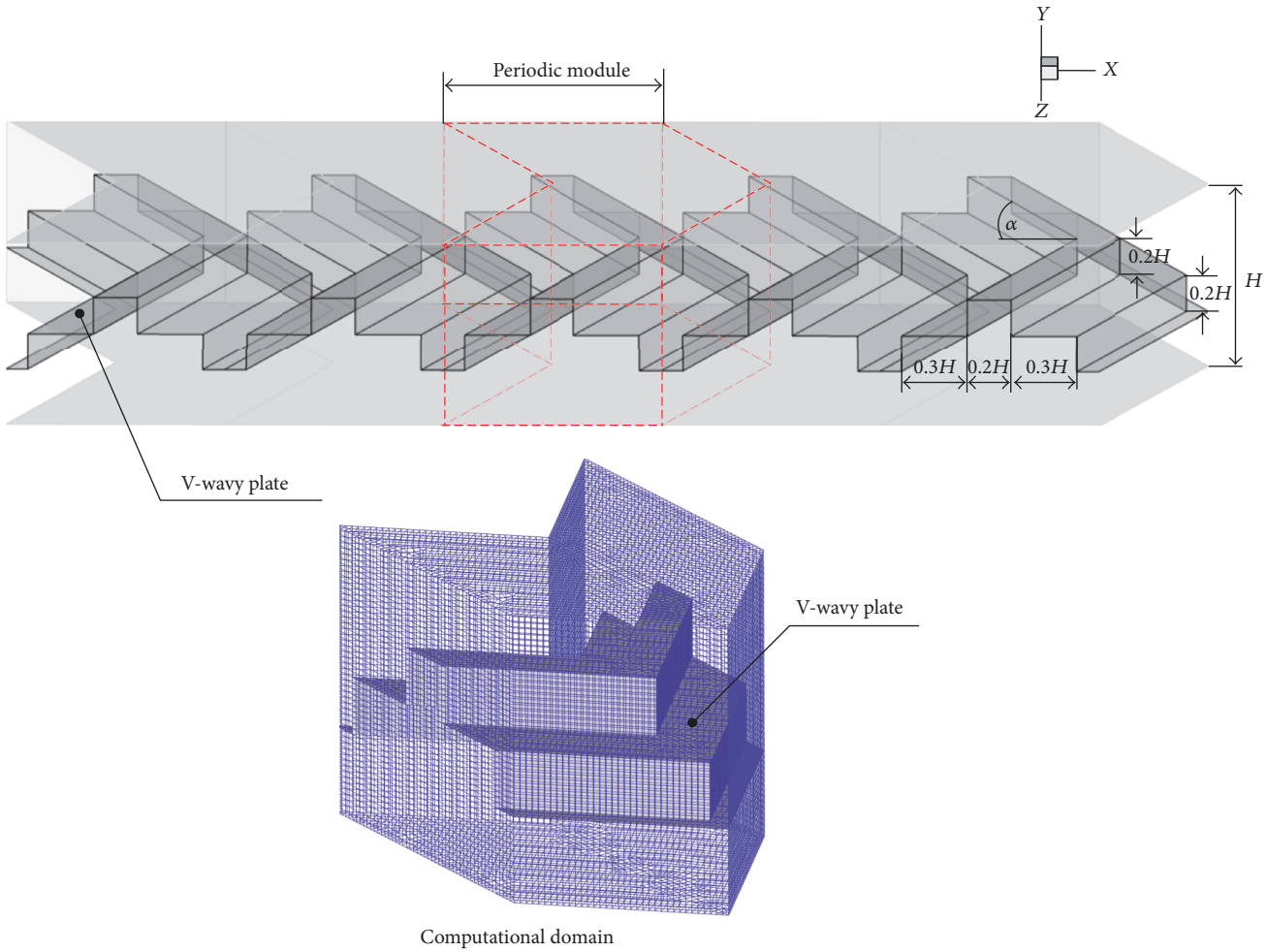

FIGURE 1: Square channel heat exchanger inserted with V-wavy plate and computational domain.

the constants in the model are given as follows:

$$\begin{aligned} C_{1\varepsilon} &= 1.44, \\ C_2 &= 1.9, \\ \sigma_k &= 1.0, \\ \sigma_\varepsilon &= 1.2. \end{aligned} \tag{3}$$

The SOU numerical scheme is selected for all governing equations, decoupling with the SIMPLE algorithm using a finite volume method (FLUENT commercial code). The solutions are considered to be converged when the normalized residual is less than 10^{-9} and 10^{-5} for the energy equation and the other variables, respectively.

The important parameters are Reynolds number (Re), friction factor (f), Nusselt number (Nu), and thermal enhancement factor (TEF).

The Reynolds number is computed from

$$\mathrm{Re} = \frac{\rho u_0 H}{\mu}. \tag{4}$$

ρ, μ, and u_0 are density, viscosity, and inlet velocity of the fluid, respectively, while H is the hydraulic diameter/height of the square channel.

The pressure loss in the heating channel is presented as friction factor. The friction factor can be calculated

$$f = \frac{(\Delta P/L)\, D_h}{2\rho \overline{u}^2}. \tag{5}$$

ΔP is the pressure drop across the periodic module, L, and u is mean flow velocity.

The heat transfer rate in the tested section is shown in terms of Nusselt number.

The local Nusselt number is computed by

$$\mathrm{Nu}_x = \frac{h_x D_h}{k}. \tag{6}$$

h_x is local heat transfer coefficient based on bulk temperature and k is thermal conductivity of the air.

The average Nusselt number can be printed by

$$\mathrm{Nu} = \frac{1}{A} \int \mathrm{Nu}_x dA, \tag{7}$$

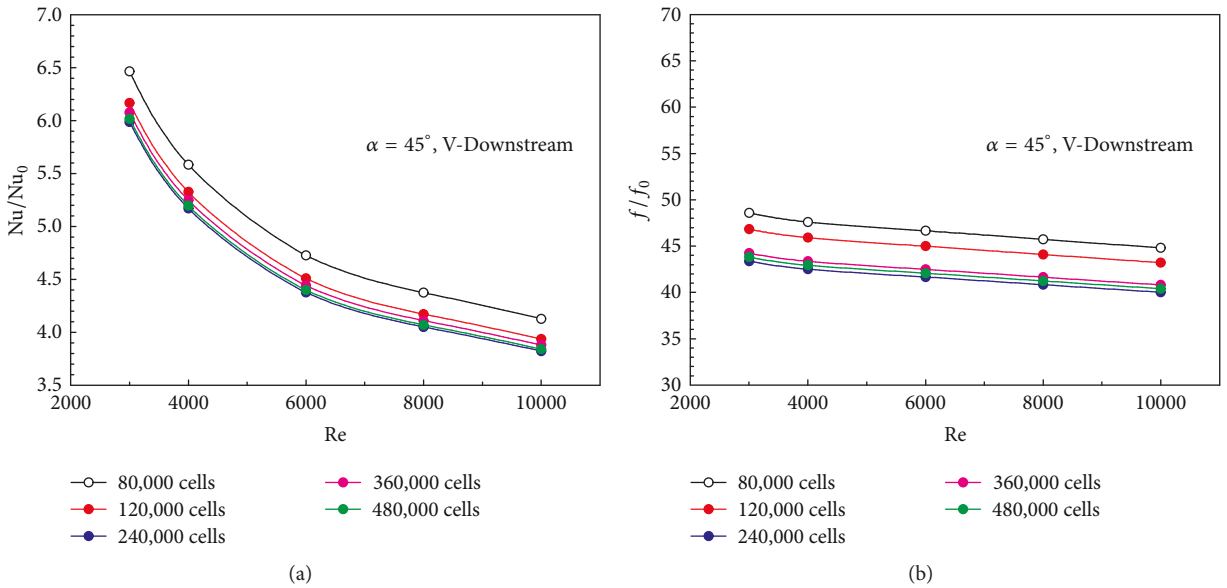

FIGURE 2: Grid independence for (a) Nusselt number and (b) friction factor of 45° V-wavy plate for V-Downstream.

where A is heat transfer area of the square channel heat exchanger.

Thermal performance is presented in the form of thermal enhancement factor (TEF).

The TEF is defined as the ratio of the heat transfer coefficient of an augmented surface, h, to that of a smooth surface, h_0, under the constant pumping power condition. The TEF can be stated as follows:

$$\text{TEF} = \frac{(\text{Nu}/\text{Nu}_0)}{(f/f_0)^{1/3}}. \tag{8}$$

4. Numerical Result

Numerical results for the present problem are separated into three parts: verification of the computational domain, mechanisms in the test section, and thermal performance analysis.

4.1. Verification of the Computational Domain. Hexahedral mesh is selected for the numerical domain. The different numbers of grids for the computational domain (α = 45°, V-Downstream) are compared as Figures 2(a) and 2(b) for Nusselt number and friction factor, respectively. As the figures, the grid around 240000, 360000, and 480000 performs similar values on both heat transfer and friction loss. Therefore, the 240000-grid cell is applied for all cases of the present research when considering the time for investigation and accuracy of the solution.

The heat transfer rate and pressure loss in the smooth channel heat exchanger for the current problem are compared with the values from the correlations as in Figure 3. From the figure, the deviations of the heat transfer and friction loss are detected within ±3%.

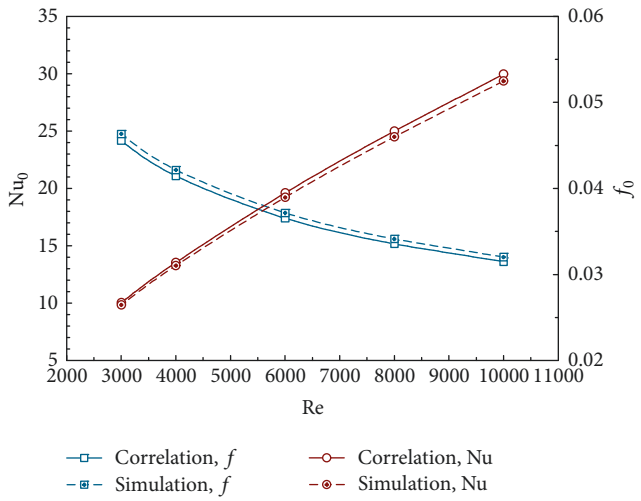

FIGURE 3: Verification of the smooth channel on Nusselt number and friction factor.

From the preliminary study, it can be concluded that the computational domain of the present study has reliability to predict flow and heat transfer in the square channel heat exchanger inserted with various flow attack angles of the V-wavy plate.

4.2. Flow and Heat Transfer Mechanisms. Figures 4(a) and 4(b) illustrate tangential velocity vector in transverse planes at various x/H positions in the square channel heat exchanger inserted with 45° wavy plate for V-Downstream and V-Upstream, respectively, at Re = 3000. In general, the wavy plate can induce the vortex flow or swirling flow through the test section on both cases. The vortex flow in the test section disturbs the thermal boundary layer on the heat transfer

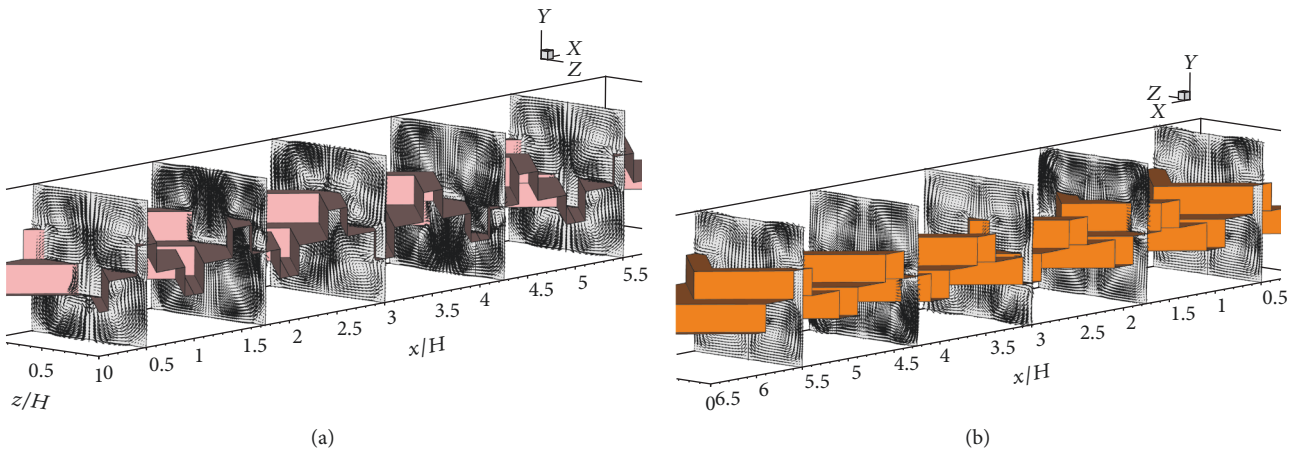

FIGURE 4: Tangential velocity vector in transverse planes of the square channel heat exchanger inserted with 45° V-wavy plate at Re = 3000 for (a) V-Downstream and (b) V-Upstream.

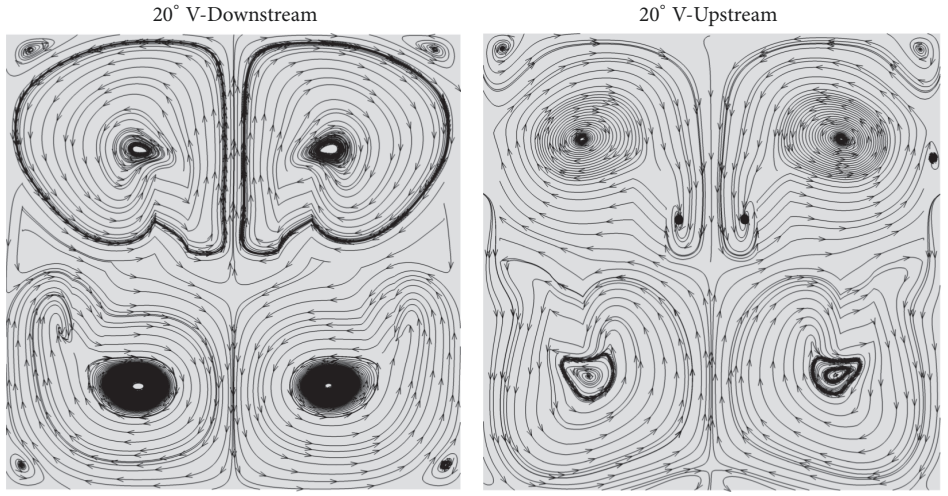

FIGURE 5: Streamline in transverse planes for the square channel heat exchanger inserted with 20° V-wavy plate at Re = 3000.

surface which is the cause of heat transfer augmentation. The flow includes four main vortex flows and small vortices at the four corners of the square channel. Considering the lower pair of the flow, the counterrotating flows with common-flow-down and common-flow-up are created from V-Downstream and V-Upstream, respectively (see Figure 5).

Figures 6(a) and 6(b) show longitudinal flow in the square channel inserted with 45° V-Downstream and V-Upstream, respectively, at Re = 3000. For V-Downstream, the air slides on the channel wall before it moves to the V-tip of the wavy surface. For V-Upstream, the air flows to the V-tip of the wavy plate and then slides to the side wall of the channel. The flow structure of the wavy plate is found in similar pattern for all flow attack angles, but the vortex strength is not equal.

Figures 7(a) and 7(b) present longitudinal swirling flow with local Nusselt number distribution on the channel wall for the square channel heat exchanger inserted with 45° wavy plate of V-Downstream and V-Upstream, respectively, at Re = 3000. The plots indicate that the swirling flow impinges on the channel wall. The impingement of the flow is the thermal boundary layer disturbance which is an important reason for heat transfer enhancement. The thermal boundary layer disturbance is detected in all sides of the square channel. For all flow attack angles and arrangements, the thermal boundary layer disturbance is detected, but the potency of the disturbance is not equal. The thermal boundary layer disturbance is also seen by the plot of temperature distribution in cross-sectional planes as depicted in Figure 8. The high temperature is plotted with red layer, while the low temperature is written with blue layer. The red layer near the channel wall is lightly found, while the blue layer is distributed from the center of the channel when inserting the wavy plate in the square channel. The temperature behavior for all flow attack angles and arrangements of the wavy plate in the square channel is found in similar pattern.

Figures 9(a) and 9(b) show local Nusselt number distribution on the channel walls of the square channel inserted with 45° wavy plate for V-Downstream and V-Upstream,

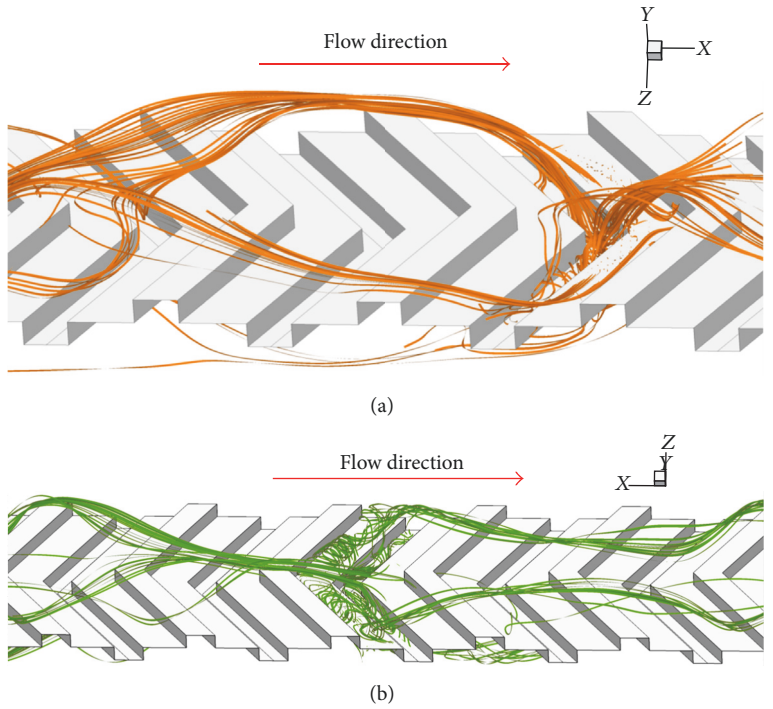

Figure 6: Longitudinal vortex flow of the square channel heat exchanger inserted with 45° V-wavy plate at Re = 3000 for (a) V-Downstream and (b) V-Upstream.

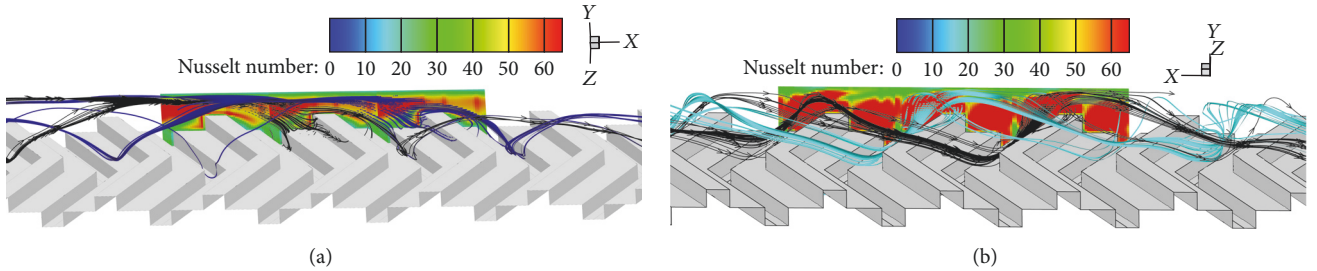

Figure 7: Impinging jet on the channel wall of the square channel heat exchanger inserted with 45° V-wavy plate at Re = 3000 for (a) V-Downstream and (b) V-Upstream.

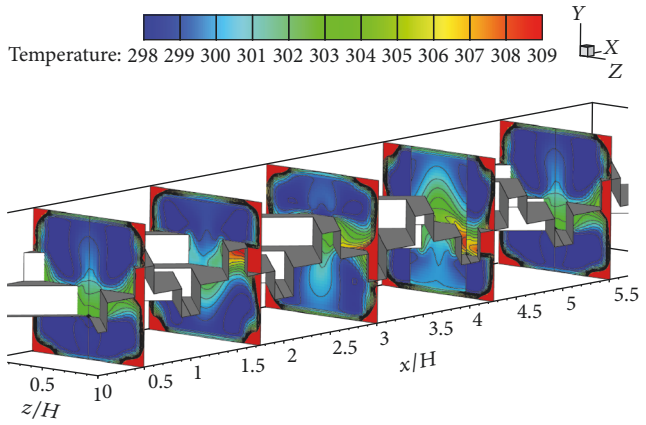

Figure 8: Temperature distribution in transverse planes for the square channel heat exchanger inserted with 45° wavy plate at Re = 3000 for V-Downstream.

respectively, at Re = 3000. In general, the insertion of the wavy plate improves the heat transfer rate higher than the smooth channel with no wavy plate. The figures indicate that the disturbance of the thermal boundary layer appears in all heat transfer surfaces. The heat transfer behavior of the V-Downstream and V-Upstream is not similar due to the different flow pattern. The peak of heat transfer rate is clearly found at the upper-lower walls of the square channel for V-Downstream. The disturbance of the thermal boundary layer is equally found in all sidewalls of the channel for the V-Upstream. The heat transfer characteristic is likely detected for all Re and α.

4.3. Thermal Performance Analysis. Figures 10(a) and 10(b) plot the relation of the Nu/Nu_0 and flow attack angle of the square channel inserted with wavy plate for V-Downstream and V-Upstream, respectively. In general, the addition of the

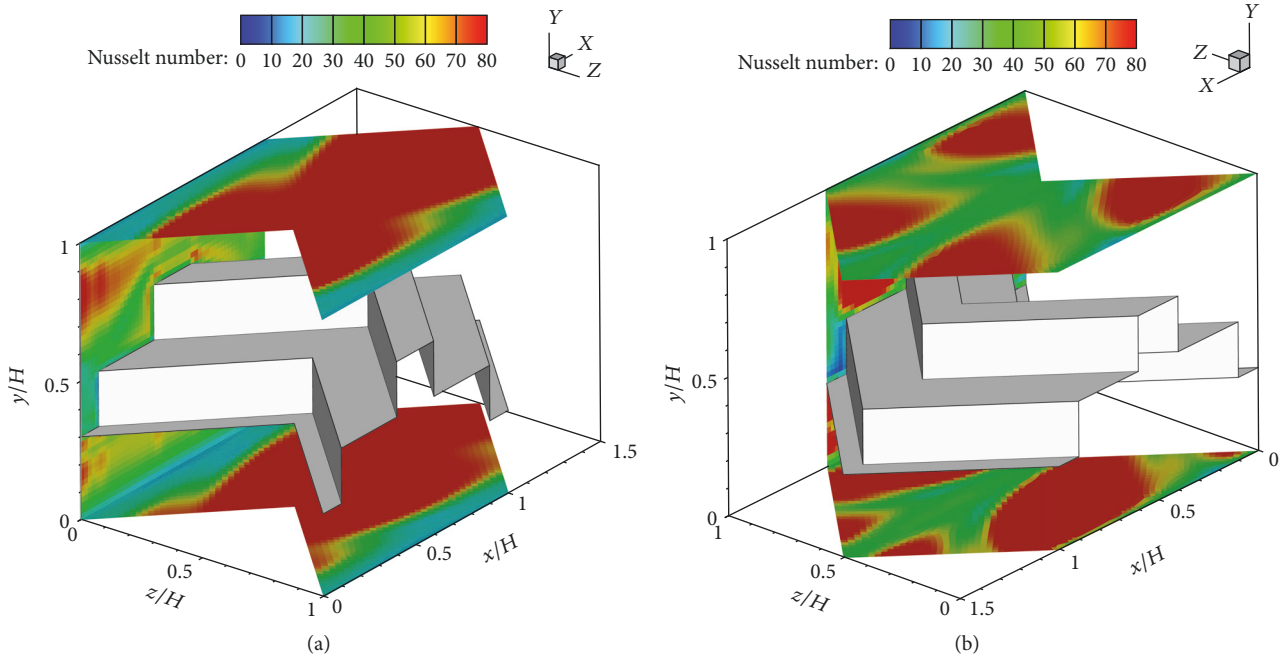

FIGURE 9: Local Nusselt number distribution on the wall surface of the square channel heat exchanger inserted with 45° V-wavy plate at Re = 3000 for (a) V-Downstream and (b) V-Upstream.

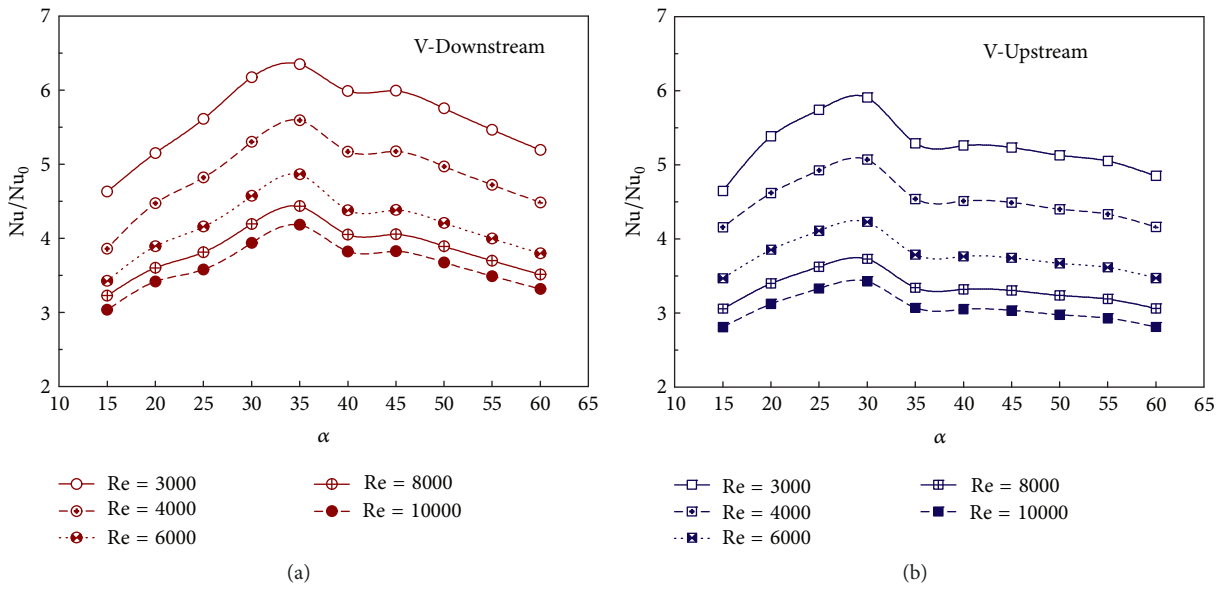

FIGURE 10: Nu/Nu_0 versus α for the square channel inserted with V-wavy plate at various Reynolds numbers of (a) V-Downstream and (b) V-Upstream.

wavy plate in the test section can improve the heat transfer rate higher than the smooth channel in all cases ($Nu/Nu_0 > 1$). Nu/Nu_0 increases when increasing the Reynolds number. For V-Downstream, $15^\circ \leq \alpha \leq 35^\circ$, the heat transfer rate tends to increase when augmenting the flow attack angle. The heat transfer rate slightly decreases when $\alpha > 35^\circ$. For V-Upstream, $15^\circ \leq \alpha \leq 30^\circ$, the Nusselt number trends to increase when enhancing the flow attack angle. The heat transfer rate slightly reduces when $\alpha > 30^\circ$. The peak of Nu/Nu_0 is detected at the flow attack angle of 35° and 30° wavy plate for V-Downstream and V-Upstream, respectively. In range studies, the Nusselt number is around 3–6.5 and 2.8–6 times above the smooth channel with no wavy plate for V-Downstream and V-Upstream, respectively.

The variation of the f/f_0 with the flow attack angle for the square channel heat exchanger inserted with wavy plate

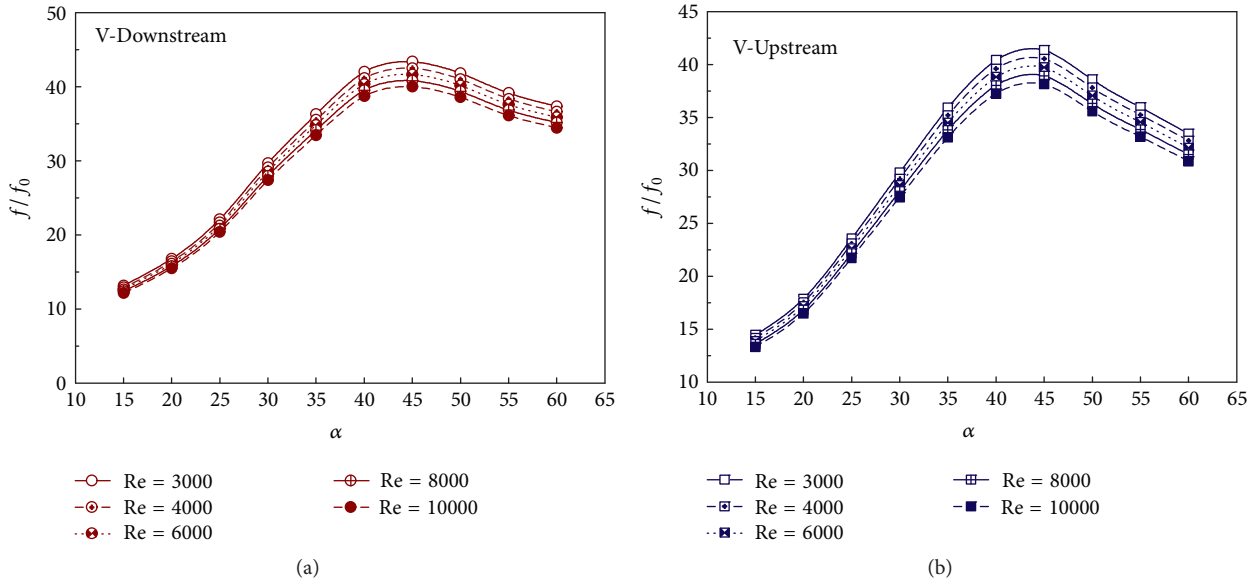

FIGURE 11: f/f_0 versus α for the square channel inserted with V-wavy plate at various Reynolds numbers of (a) V-Downstream and (b) V-Upstream.

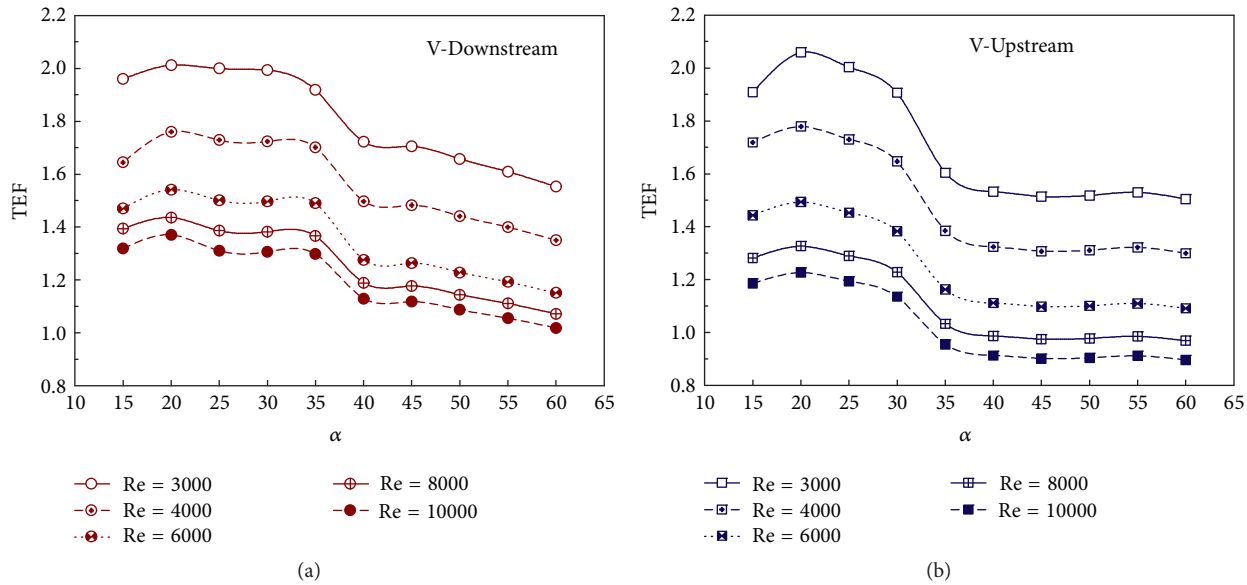

FIGURE 12: TEF versus α for the square channel inserted with V-wavy plate at various Reynolds numbers of (a) V-Downstream and (b) V-Upstream.

at various Reynolds numbers is depicted as Figures 11(a) and 11(b), respectively, for V-Downstream and V-Upstream. The insertion of the wavy plate in the square channel enhances the friction loss higher than the plain channel for all cases ($f/f_0 > 1$). Similar trend of the friction factor is found for both arrangements. The friction loss reduces when augmenting the Reynolds number. In range, $15^\circ \leq \alpha \leq 45^\circ$, the friction loss increases when increasing the flow attack angle. The friction factor tends to decrease when $\alpha > 45^\circ$. The wavy plate with 45° performs the highest friction loss, while the wavy plate with 15° gives the reverse result. The wavy plate with V-Downstream provides the friction loss higher than the smooth channel around 11–44 times but around 15–42 times for V-Upstream.

Figures 12(a) and 12(b) show the relation of the TEF with the flow attack angle at various Reynolds numbers for the square channel heat exchanger inserted with wavy plates for V-Downstream and V-Upstream, respectively. The TEF decreases when increasing the Reynolds number. The optimum TEF is detected at the flow attack angle around 20° for both arrangements. The TEF is around 2.02 and 2.09 for V-Downstream and V-Upstream, respectively, at Re = 3000.

5. Conclusion

Numerical prediction on flow and heat transfer mechanisms in the square channel inserted with V-wavy plate is presented. The influences of the flow attack angles ($\alpha = 15^\circ, 20^\circ, 25^\circ, 30^\circ, 35^\circ, 40^\circ, 45^\circ, 50^\circ, 55^\circ$, and 60°) and V-tip arrangements (V-Downstream and V-Upstream) are investigated for turbulent regime (Re = 3000–10,000). The major findings for the present investigation are as follows:

(i) The addition of the wavy plate in the test section leads to producing the vortex flow or swirling flow through the test section. The vortex flow is an important factor for heat transfer improvement in the heating section because the vortex flow disturbs the thermal boundary layer on the channel walls. The insertion of the wavy plate not only increases in heat transfer rate, but also enhances the pressure loss.

(ii) The maximum heat transfer rate is detected at the flow attack angle around 35° and 30° of the wavy plate for V-Downstream and V-Upstream, respectively. The wavy plate with V-Downstream and V-Upstream performs the heat transfer rate higher than the smooth channel around 3–6.5 and 2.8–6 times, respectively, for $\alpha = 15^\circ$–60° and Re = 3000–10,000.

(iii) The friction loss of the square channel inserted with the wavy plate is found to be maximum at the flow attack angle around 45°, while the flow attack angle of 15° performs the opposite result for both cases. In range studies, the friction loss is higher than the smooth channel around 11–44 times.

(iv) The optimum TEF is found at 20° wavy plate to be about 2.02 and 2.09, respectively, for V-Downstream and V-Upstream.

(v) The manufacture and installation of the V-wavy plate is more convenient than other types of the turbulators such as V-baffle placed on the channel wall.

(vi) The optimum flow attack angles of the wavy surface in the heat exchanger channel for laminar [17] and turbulent flow are 40° and 20°, respectively, when considered at the thermal enhancement factor.

Nomenclature

f: Friction factor
H: Channel height
h: Convective heat transfer coefficient ($W/m^2 K$)
k: Thermal conductivity (W/m K)
Nu: Nusselt number
p: Static pressure (Pa)
Pr: Prandtl number
Re: Reynolds number
T: Temperature (K)
TEF: Thermal enhancement factor
u_i: Velocity in xi-direction (m/s)
$\overline{u}$: Mean velocity in channel (m/s)
x, y, z: Cartesian coordinates.

Greek Symbols

α: Flow attack angle, degree
μ: Dynamic viscosity (Pa s)
ρ: Density (kg/m^3)
Γ: Thermal diffusivity.

Subscripts

in: Inlet
w: Wall
0: Smooth tube.

Conflicts of Interest

The authors declare that there are no conflicts of interest regarding the publication of this article.

Acknowledgments

The funding of this work is supported by King Mongkut's Institute of Technology Ladkrabang research funds (Contract no. KREF046006). The authors would like to thank Associate Professor Dr. Pongjet Promvonge, KMITL, for suggestions.

References

[1] R. Kumar, R. Chauhan, M. Sethi, and A. Kumar, "Experimental study and correlation development for Nusselt number and friction factor for discretized broken V-pattern baffle solar air channel," *Experimental Thermal and Fluid Science*, vol. 81, pp. 56–75, 2017.

[2] W. Jedsadaratanachai, N. Jayranaiwachira, and P. Promvonge, "3D numerical study on flow structure and heat transfer in a circular tube with V-baffles," *Chinese Journal of Chemical Engineering*, vol. 23, no. 2, pp. 342–349, 2015.

[3] W. Jedsadaratanachai and A. Boonloi, "Effects of blockage ratio and pitch ratio on thermal performance in a square channel with 30◦ double V-baffles," *Case Studies in Thermal Engineering*, vol. 4, pp. 118–128, 2014.

[4] S. Caliskan and S. Baskaya, "Velocity field and turbulence effects on heat transfer characteristics from surfaces with V-shaped ribs," *International Journal of Heat and Mass Transfer*, vol. 55, no. 21-22, pp. 6260–6277, 2012.

[5] D. Jin, J. Zuo, S. Quan, S. Xu, and H. Gao, "Thermohydraulic performance of solar air heater with staggered multiple V-shaped ribs on the absorber plate," *Energy*, vol. 127, pp. 68–77, 2017.

[6] N. S. Deo, S. Chander, and J. S. Saini, "Performance analysis of solar air heater duct roughened with multigap V-down ribs combined with staggered ribs," *Journal of Renewable Energy*, vol. 91, pp. 484–500, 2016.

[7] P. Promthaisong, P. Eiamsa-ard, W. Jedsadaratanachai, and S. Eiamsa-ard, "Turbulent heat transfer and pressure loss in a square channel with discrete broken V-rib turbulators," *Journal of Hydrodynamics, Series B*, vol. 28, no. 2, pp. 275–283, 2016.

[8] X. Fang, Z. Yang, B.-C. Wang, M. F. Tachie, and D. J. Bergstrom, "Highly-disturbed turbulent flow in a square channel with V-shaped ribs on one wall," *International Journal of Heat and Fluid Flow*, vol. 56, pp. 182–197, 2015.

[9] R. Maithani and J. S. Saini, "Heat transfer and friction factor correlations for a solar air heater duct roughened artificially with V-ribs with symmetrical gaps," *Experimental Thermal and Fluid Science*, vol. 70, pp. 220–227, 2016.

[10] D. Jin, M. Zhang, P. Wang, and S. Xu, "Numerical investigation of heat transfer and fluid flow in a solar air heater duct with multi V-shaped ribs on the absorber plate," *Energy*, vol. 89, pp. 178–190, 2015.

[11] B. Lotfi, M. Zeng, B. Sundén, and Q. Wang, "3D numerical investigation of flow and heat transfer characteristics in smooth wavy fin-and-elliptical tube heat exchangers using new type vortex generators," *Energy*, vol. 73, pp. 233–257, 2014.

[12] J. Dong, L. Su, Q. Chen, and W. Xu, "Experimental study on thermal-hydraulic performance of a wavy fin-and-flat tube aluminum heat exchanger," *Applied Thermal Engineering*, vol. 51, no. 1-2, pp. 32–39, 2013.

[13] J. Dong, J. Chen, W. Zhang, and J. Hu, "Experimental and numerical investigation of thermal -hydraulic performance in wavy fin-and-flat tube heat exchangers," *Applied Thermal Engineering*, vol. 30, no. 11-12, pp. 1377–1386, 2010.

[14] J. Gong, C. Min, C. Qi, E. Wang, and L. Tian, "Numerical simulation of flow and heat transfer characteristics in wavy fin-and-tube heat exchanger with combined longitudinal vortex generators," *International Communications in Heat and Mass Transfer*, vol. 43, pp. 53–56, 2013.

[15] X. Du, L. Feng, L. Li, L. Yang, and Y. Yang, "Heat transfer enhancement of wavy finned flat tube by punched longitudinal vortex generators," *International Journal of Heat and Mass Transfer*, vol. 75, pp. 368–380, 2014.

[16] X. Du, L. Feng, Y. Yang, and L. Yang, "Experimental study on heat transfer enhancement of wavy finned flat tube with longitudinal vortex generators," *Applied Thermal Engineering*, vol. 50, no. 1, pp. 55–62, 2013.

[17] A. Boonloi and W. Jedsadaratanachai, "Laminar forced convection and heat transfer characteristics in a square channel equipped with V-wavy surface," *Journal of Mathematics and Statistics*, vol. 13, no. 3, pp. 251–260, 2017.